

RESEARCH PAPER



A fast, miniaturised *in-vitro* assay developed for quantification of lipase enzyme activity

Ariane Menden^{a,b} , Davane Hall^a , Daniel Paris^{a,b}, Venkatarian Mathura^a , Fiona Crawford^{a,b}, Michael Mullan^{a,b} , Stefan Crynen^{a,b} and Ghania Ait-Ghezala^{a,b} 

^aDepartment of Genomics, Roskamp Institute, Sarasota, FL, USA; ^bARC, Open University, Milton-Keynes, United Kingdom

ABSTRACT

The discovery of allosteric modulators is a multi-disciplinary approach, which is time- and cost-intensive. High-throughput screening combined with novel computational tools can reduce these factors. Thus, we developed an enzyme activity assay, which can be included in the drug discovery work-flow subsequent to the *in-silico* library screening. While the *in-silico* screening yields in the identification of potential allosteric modulators, the developed *in-vitro* assay allows for the characterisation of them. *Candida rugosa* lipase (CRL), a glyceride hydrolysing enzyme, has been selected for the pilot development. The assay conditions were adjusted to CRL's properties including pH, temperature and substrate specificity for two different substrates. The optimised assay conditions were validated and were used to characterise Tropolone, which was identified as an allosteric modulator. In conclusion, the assay is a reliable, reproducible, and robust tool, which can be streamlined with *in-silico* screening and incorporated in an automated high-throughput screening workflow.

ARTICLE HISTORY

Received 8 May 2019
Revised 25 July 2019
Accepted 26 July 2019

KEYWORDS


Candida rugosa lipase; hydrolase; enzyme activity assay; lipase inhibitor; Tropolone

1. Introduction

Lipases or triacylglycerol acyl hydrolases (EC 3.1.1.3) catalyse the hydrolysis of triacyl glycerides to release fatty acids and glycerol, an established mechanism in yeast. They comprise a broad variety of lipase structures with common structural traits¹. Yeasts' secretion of lipases support their establishment in plants by hydrolysing epicuticular waxes, which enables access to nutrition and carbohydrates in the roots of plants as a survival mechanism². *Candida rugosa* is an especially potent species that secretes 5 isoforms of lipases with an identity of 77%. Despite their structural similarity, the five isoforms of *Candida rugosa* lipase (CRL) covers a broad specificity range in catalysing the breakdown of lipids into fatty acids and glycerol³; which is also the reason why this subset is widely used in the industry, for instance, in the production of biodiesel and pharmaceuticals^{4,5}. This broad specificity range enables *Candida rugosa* to hydrolyse fatty acids preferentially from position 1 or 3 on the glyceride with an additional preference for medium- and long-chain fatty acid, but no preference between saturated and unsaturated fatty acids as well as cholesterol^{6–8}. The varying specificity within the isoforms is caused by sequential differences in a conserved loop and tunnel domain, which determines the activity and specificity of the respective isoforms^{7,9,10}. The loop is composed of an α -helix in the closed conformation, where it lays planar on the molecule's surface covering the catalytic centre (catalytic triad: Ser209-His449-Glu341, a water molecule, and the oxyanion hole) as well as the tunnel entrance inhibiting catalytic activity^{11,12}. For the transition in the open conformation, the respective loop has to travel 19 Å, positioning itself perpendicular to the enzyme's surface exposing the catalytic

centre and the tunnel entrance and refolding itself into two α -helices^{11,12}. One of the acyl groups on the glyceride can subsequently move into the accessible tunnel domain, which contains several functional groups stabilising the hydrophobic acyl chain. This positions the ester bond connecting the fatty acid and glycerol in the catalytic centre, initiating the hydrolysis activity and subsequently releasing a free fatty acid as well as diacylglyceride¹¹. Changes in the sequence by site-directed mutation of both the loop and the tunnel domain can have effects on specificity and activity of the enzyme^{7,13}. In addition, it was discovered that CRL isoforms' activity is very sensitive to pH and temperature changes^{4,14}. While the application of immobilisation strategies as well as the addition of hydrophobic organic solvents or emulsions showed to enhance the enzyme's activity by stabilising the exposed hydrophobic areas in the open conformation^{15–18}, certain experimental conditions can even change the direction of the catalytic reaction, meaning an ester bond formation instead of hydrolysis¹⁹. Although allosteric modulation is very effective and is a biochemical method to alter enzymatic activity and specificity, it has not been considered in the past due to the mentioned alternative procedures, complexity and cost-intensity of high-throughput screening with numerous potential modulators. In modern approaches, the identification of allosteric sites is simplified through pre-screening of potential allosteric modulators by computational analysis, which pre-sorts and reduces the pool of screening component as well as complexity and cost-intensity^{20–22}. However, *in-silico* based screening requires an X-ray-crystallography structure of the respective enzyme as well as high-performance software and hardware, an *in-vitro* screening assay, which can

CONTACT Ariane Menden  amenden@roskampinstitute.org  2040 Whitfield Avenue, Sarasota, FL, 34243, USA

 Supplemental data for this article can be accessed [here](#).

© 2019 The Author(s). Published by Informa UK Limited, trading as Taylor & Francis Group.

This is an Open Access article distributed under the terms of the Creative Commons Attribution-NonCommercial License (<http://creativecommons.org/licenses/by-nc/4.0/>), which permits unrestricted non-commercial use, distribution, and reproduction in any medium, provided the original work is properly cited.

verify the theoretically determined ligands and their influence on the enzyme's activity.

Therefore, we developed a rapid, miniaturised, high-throughput assay starting from Dairaku et al.'s proposed method²³, which can be used as *in-vitro* identification tool in existing *in-silico* workflows elucidating the impact of *in-silico* determined ligands on the enzyme's activity. The assay is reproducible, reliable, and enables flexible adjustments depending on the enzyme's specificity and enzyme class. For the assay's development, *Candida rugosa* lipase isoforms were selected due to the availability of their X-ray crystallography structure (PDB: 1CRL, 1TRH) and their wide use in industrial production processes.

2. Materials and methods

2.1. Materials

Candida rugosa lipase was received from Deerland (Kennesaw, GA, USA). 4-Methylumbelliferyl palmitate (4-MUP) and Trigonelline were obtained from Cayman Chemicals (Ann Arbor, MI, USA). 4-Methylumbelliferyl (4-MU), 4-Methylumbelliferyl butyrate (4-MUB), dimethyl sulfoxide (DMSO), sodium phosphate dibasic heptahydrate, sodium phosphate monobasic monohydrate, Tropolone and Berberine were purchased from Sigma Aldrich (St. Louis, MO, USA). β -Aescin was purchased from Santa Cruz Biotechnology (Dallas, TX, USA). 85% o-phosphoric acid was received from Fisher Scientific (Waltham, MA, USA). Sterile, black, μ CLEAR, flat bottom, 96-well plates were obtained from VWR (Radnor, PA, USA).

2.2. Enzyme activity assay

Standards and samples were measured in triplicates in a black, μ -clear bottom 96-well plate. Dilutions and blanks were prepared with 0.1 M phosphate buffer pH 7. The standard curve was prepared with a 400 μ M stock of 4-MU in DMSO and 0.1 M phosphate buffer (pH 7.0) with a range of 7.813 μ M to 500 μ M (final: 1.95–62.5 μ M). 50 μ L buffer and 50 μ L of standard solution was added to respective standard wells, while 100 μ L buffer were added to the blank wells. 50 μ L of CRL at 10 ng/mL (final concentration: 2.5 ng/mL) for 4-MUB or 50 ng/mL CRL (final concentration 12.5 ng/mL) for 4-MUP and 50 μ L of buffer or additive (enhancer, inhibitor) were added to the respective sample wells. A 10 mM stock of 4-MUB and 10 mM stock of 4-MUP were prepared in DMSO and diluted in buffer (4-MUB) or buffer and 0.006% SDS (*w/v*) incubated at 37 °C (4-MUP) to a concentration of 0.25 mM. 50 μ L of 4-MUB and 150 μ L of 4-MUP were added to each well. The 96-well plate was incubated at 37 °C for 25 min. The reaction was stopped with 50 μ L of 10% o-phosphoric acid in MilliQ water for 4-MUB and 10 μ L for 4-MUP. The fluorescence was immediately measured with the BioTek Cytation 3 system at $\lambda = 326/472$ with a gain of 72.

2.3. Validation of enzyme activity assay

Blank and standards were diluted and prepared as described in the enzyme activity section 2.2. Samples were run in triplicates containing CRL in buffer, CRL with 200 μ M 4-MU (final: 50 μ M 4-MU) and CRL with 12.5 μ M 4-MU (final: 3.125 μ M 4-MU). The experiment was executed over three consecutive days to determine intra- and inter-day CV for all three samples as well as intra- and inter-day precision for both spiked reactions.

2.4. Temperature and pH stability of enzyme activity assay

Robustness of the assay conditions was tested by performing the assay at a different temperature or pH conditions according to the protocol in Section 2.2.

2.4.1. Temperature

The standard curve was prepared in triplicates and several plates incubated at different temperatures including enzyme plus substrate and blank samples in triplicates for each temperature point (4 °C, 15 °C, 25 °C, 28 °C, 37 °C, 45 °C). Each sample was corrected for their individual blank at the respective temperature.

2.4.2. pH

Sample containing the enzyme plus substrate and blank were also run in duplicates for each pH. Reaction conditions were otherwise maintained as described above in the assay protocol.

2.5. Stability of CRL in water

CRL (1 mg/mL) was incubated in water for six days at room temperature. Samples were collected at day 0, 1, 3, 5, and 6. Subsequently, the collected samples were analysed on a stain-free SDS gel and with the 4-MUB activity assay according to Section 2.2 to investigate changes of activity and quantity.

2.6. Inhibitor analysis

The *in-silico* determined inhibitor Tropolone was identified with the CRL1 structure (PDB: 1CRL) and the compiled ligand screen from the Zinc database (Zbc; Zbc Leads; Zbc Drugs; Zbc frags), InterBioScreen database (natural compounds) and AnalytiCon database (FRGx, MEGx) (supplementary method S1). Tropolone's impact on CRL was analysed by determining the IC₅₀ with both substrates (4-MUB and 4-MUP) according to the described protocol in Section 2.2. A 1 M Tropolone stock was prepared in DMSO and diluted in phosphate buffer pH 7 to a final concentration range of 2 μ M to 10 mM in the reaction and compared to CRL without inhibitor addition. In addition, Berberine's, Trigonelline's and β -Aescin's IC₅₀ were analysed and compared to Tropolone. Tested concentration ranges were based on published IC₅₀'s and required CRL's concentration being reduced 10-fold.

2.7. Michaelis–Menten kinetics

K_m and V_{max} were determined by measuring eight different substrate concentration at six-time points. Each concentration at each time point had a separate blank. The plot of time vs. concentration of fluorescent dye for each substrate concentration determined V₀ (slope of linear graph) for each substrate concentration. V₀ values were subsequently plotted against the substrate concentration based on the Michaelis–Menten plot to calculate K_m and V_{max}

$$V_0 = \frac{V_{\max} \cdot [S]}{K_m + [S]} \quad (1)$$

K_m = Michaelis–Menten constant; V_{max} = maximal velocity; V₀ = initial velocity; [S] = substrate concentration.

In addition, the kinetics experiment was performed with two different Tropolone concentrations to determine the type of inhibitory activity imposed by Tropolone. All time points and

substrate concentration were maintained. Tropolone was added prior to the experiment in a concentration of 100 μM or 400 μM and K_m and V_{max} were compared.

Statistical analyses were performed for determination of K_m , V_{max} and IC_{50} using Graphpad Prism 8 (San Diego, CA, USA).

3. Results

3.1. Enzyme activity assay development

Starting with Dairaku et al.'s proposed protocol for the human lysosomal acid lipase²³, we developed an enzyme activity assay, which is applicable for two types of lipase specificities: short-chain fatty acid (butyrate) and long-chain fatty acids (palmitate). The selected substrates (4-Methylumbelliferyl butyrate (4-MUB) and palmitate (4-MUP)) comprise these fatty acids connected to the fluorescent dye 4-MU via an ester bond, respectively. 4-MU emits fluorescence upon hydrolysis of the ester bond and excitation at the corresponding wavelength. While 4-MUB is stable in phosphate buffer (pH 7.0), 4-MUP requires an additional stabilising agent (SDS) for the hydrophobic longer-chain fatty acid palmitate in aqueous solution (37 °C). To translate the subsequent fluorescence emitted by 4-MU after CRL hydrolysis of the substrate into concentration units, a seven-point standard curve of defined 4-MU concentrations was included ranging from 1.563 to 62.5 μM diluted in assay buffer. The curve (Figure 1(A)) is linear within the defined range (Figure 1(B)) and was analysed with a linear regression fit. The standard curve allows the translation of relative fluorescent units into concentration (μM) within the Lower Limit of Quantification (LLOQ) of 0.5 μM 4-MU and the Upper Limit of Quantification of 62.5 μM .

Subsequently, several parameters were adjusted separately for both substrates. While the concentration of the substrate was

constant in both assays (250 μM), the concentration of the enzyme was adjusted to account for SDS's inhibitory effect on CRL (data not shown). Therefore, the 4-MUP assay required 10 ng/mL, while the 4-MUB assay's concentration needed to be reduced to 3.3 ng/mL CRL (Supplementary Figure S3). Furthermore, it was determined that 10 μL and 50 μL of 10% o-H₃PO₄ was sufficient to completely stop the reaction for 4-MUB and 4-MUP, respectively (Supplementary Figure S1). Moreover, accuracy and precision for each substrate were evaluated separately over three-day, (Table 1), which confirmed reproducibility and comparability of measurements within the assay and between days.

3.2. Assay robustness

Although the assay was validated for both substrates, our data shows superior aqueous solubility of 4-MUB as compared to 4-MUP requiring the use of SDS, which inhibits the enzyme's activity (Supplementary Figure S3). Thus, we focussed on the substrate 4-MUB for further determination of validation parameters to avoid interference with the enzyme's activity. Subsequently, we investigated the assay performance with 4-MUB at different temperatures (Figure 2(A)) and pHs (Figure 2(B)).

Five different temperatures, 4, 15, 28, 37 and 45 °C were tested. Our data indicated that the enzyme is temperature sensitive and most active between 37–45 °C as the optimal temperature for the enzyme activity. However, 37 °C was maintained for further experiments as it represents physiological conditions. The investigation of the reaction's efficiency at six different buffer pH revealed the stability of the enzyme's activity in lower pH ranges and increased instability of the assay above pH 8. Under basic conditions, the substrate is subject to autohydrolysis, making the reaction independent of the enzyme's activity and which is characteristic for ester bonds. Therefore, the selected reaction conditions were approximated to physiological conditions at pH 7, since they show the robustness and optimal reaction requirements.

3.3. Analysis of CRL extract

The used enzyme extract CRL, obtained from Deerland was further characterised. First, we investigated, which of the isoforms were present in the extract and second, which other components could be present in the mixture. A gas-chromatography analysis (GCMS) revealed the presence of only CRL isoforms 1, 2, 3, and 4, although 4 had solely one fragment detected indicating a low abundance (see Supplementary Table S1). Furthermore, the stability of the enzyme in water was determined over six days at room temperature to identify potential impurities degrading the enzyme in solution (Figure 3).

Our data showed that both methods, SDS page and GCMS, revealed a pure enzyme extract, which was used for the investigation of CRL's enzyme activity (Supplementary Figure S2 and Supplementary Table S1). However, the activity assay showed a slightly decreasing activity over the six-day period indicating auto-degradation or presence of proteases that were below the detection limit of the method used for evaluation. Thus, the identification of mainly the 4 isoforms of CRL in the extract and only a slight degradation over 6 days, deemed the enzyme extract to be pure and stable in water.

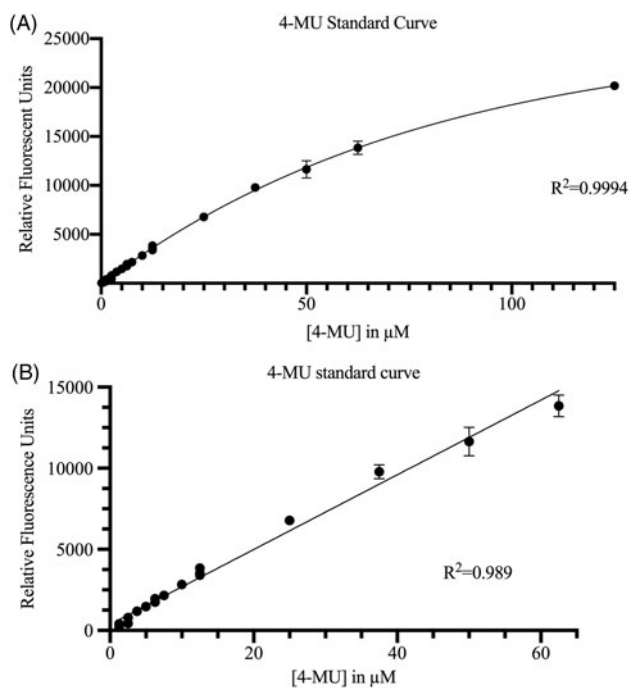
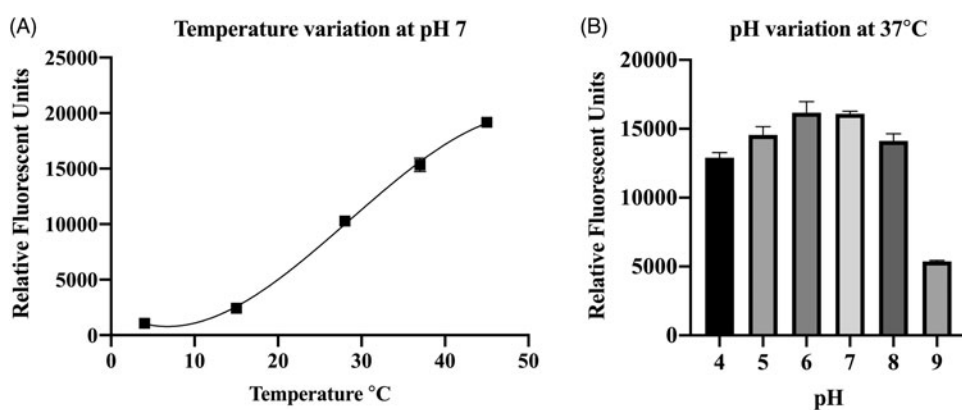


Figure 1. 4-MU standard curve. (A) Plot of several 4-MU concentrations (0.125–125 μM) to determine the shape of the standard curve. The sigmoidal shape was analysed with a 4-parameter logistic fit. (B) The linear range for the standard curve was determined between the Lower Limit of Quantification (LLOQ) and Upper Limit of Quantification (ULOQ), which is in the linear range at concentrations ranging from 0.5 to 62.5 μM .

Table 1. Validation of the enzyme activity assay for both substrates 4-MUB (A) and 4-MUP (B). Samples were measured in triplicates each day allowing to determine Precision (Intra-Day and Inter-Day CV%) and Accuracy (%) for the validation.

A				
Analytes (Substrate: 4-MUB)	Concentration (μM) ($n = 3$)	Precision (CV) (%)		Accuracy (%) ($n = 3$)
		Intra-day ($n = 3$)	Inter-day ($n = 3$)	
QC1 ^a	12.8 \pm 0.6	0.5–6.5	4.6	
QC2 ^b	16.7 \pm 1.2	1.3–3.3	6.9	0.7%
QC3 ^c	74.2 \pm 3.2	0.9–2.6	4.4	1.7%
B				
Analytes (Substrate: 4-MUP)				
QC1 ^a	6.5 \pm 0.4	0.9–2.2	5.6	
QC2 ^b	9.8 \pm 0.6	0.6–4.2	6.0	2.0%
QC3 ^c	56.8 \pm 1.9	0.8–2.6	3.4	0.6%

^aQC1: CRL and substrate.^bQC2: CRL, substrate and a low spike of 4-MU (3.13 μM).^cQC3: CRL, substrate and a high spike of 4-MU (50 μM).**Figure 2.** Determination of assay robustness under application of altered conditions. (A) Temperature variation (4–45 °C) with buffer pH 7. (B) Buffer pH variation (pH 4–9) with reaction temperature 37 °C.

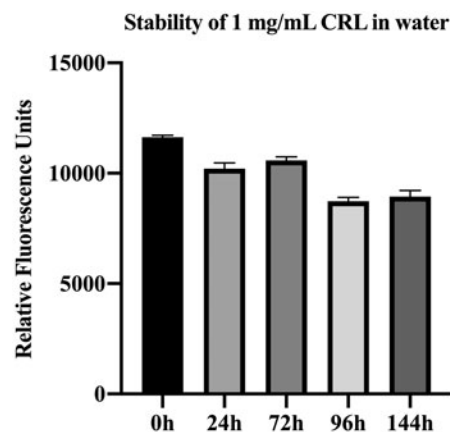
3.4. Identification of an effective inhibitor

Subsequently, we used the *in-vitro* assay to verify the allosteric modulator potential of Tropolone, a compound, which was determined in an *in-silico* screening approach (Glide, Schroedinger, XP GScore: -5.603)²⁴. Tropolone was used to demonstrate the underlying workflow (Supplementary method S1). Tropolone was investigated in both developed *in-vitro* assays in a concentration range of 2 μM to 10 mM with both substrates showing a concentration-dependent inhibition (Figure 4(A)). We calculated the corresponding IC₅₀ values (4-MUP: 3.75×10^{-4} M; 4-MUB: 3.95×10^{-4} M) by plotting the logarithmic Tropolone concentration against the activity of CRL (%), which indicates CRL's inhibition being slightly more efficient in 4-MUP samples with a lower IC₅₀ value (Figure 4(B)).

In addition, we investigated reported CRL inhibitors and their IC₅₀ values. The reduction of the concentration of CRL by 10-fold in the assay allowed the measurement of IC₅₀ values of weak inhibitors. The measured IC₅₀ values in the in-house activity assay were close to the reported IC₅₀s of Trigonelline, β -Aescin and Berberine (Supplementary Figure S4)^{25,26}.

3.5. Michaelis–Menten kinetics

Finally, we determined the kinetic parameters of the CRL extract. The in-house developed assay with the substrate 4-MUB was used

**Figure 3.** Investigation of CRL's stability throughout six days in water at room temperature. The in-house developed activity assay was applied to determine for each sampled day the impact on the enzyme's activity, which slightly decreased over time.

and applied in 8 different concentrations over a 50-min time span by measuring the increase of relative fluorescent units over time. The subsequent plot of initial velocity against the substrate concentration (Michaelis–Menten plot) allowed the determination of V_{max} (0.54 ± 0.03 $\mu\text{M}/\text{min}$) and K_m (0.46 ± 0.06 mM) for the butyrate substrate (Figure 5(A,B)).

The additional analysis of K_m and V_{max} after addition of Tropolone in two different concentrations (100 and 400 μM), respectively, determined Tropolone's mode of inhibition. While K_m did not show a clear trend of decline or increase due to inhibitor addition, V_{max} decreased with increasing inhibitor concentration (Figure 5(A,B)). This experimental trend and the analysis of the Lineweaver-Burk plot (data not shown), confirmed the *in-silico* analysis, which identified Tropolone as an allosteric modulator of CRL and identified the inhibition as non-competitive. Furthermore, we examined Trigonelline and β -Aescin together with Tropolone using biolayer-interferometry (Supplementary method S2) to investigate the binding of CRL with these compounds.

β -Aescin's K_D was determined to be relatively low but was inconsistent with high IC_{50} suggesting non-specific binding to CRL. By contrast, Tropolone's determined K_D value was consistent

with its relatively low IC_{50} (compared to β -Aescin) indicating a more specific interaction. However, the relatively modest IC_{50} is consistent with Tropolone's deemed mechanism of action, namely allosteric modulation. Finally, Trigonelline showed relatively high K_D and IC_{50} , indicating low or unspecific interaction with CRL (Supplementary Figure S5).

4. Discussion

In this study, we developed and applied an enzyme activity assay for two different substrate specificities (4-MUB (short-chain fatty acids) and 4-MUP (long-chain fatty acids)) to verify the mode of action (allosteric modulation) of Tropolone. The *in-vitro* assay conditions were validated and showed reproducibility, robustness, and stability. The assay is a reliable and cost-effective enzymatic assay tool, which is easily implemented. In particular, the consideration of a reagent to stop the reaction, which differentiates this from other published assays, is pivotal for reproducibility within and between different reads^{27,28}. Although the current assay conditions were optimised for Deerland's CRL extract, the assay allows adjustments for any enzyme's specificity as 4-MU cannot only be synthesised to other fatty acids, but also to substrates of glucosidases or phosphatases. The use of 4-MUB and 4-MUP demonstrated the assay's adaptability to different substrates. In future experiments, different fatty acids (substrates) and combinations could be investigated. However, we acknowledge the limitations of the assay such as the intrinsic decrease in solubility of the hydrophobic fatty acid tail with length and the autocatalysis of the substrate in the basic pH range.

In addition, the assay allows measurement of IC_{50} s and kinetic parameters and characterisation of the enzyme's performance. Similarly, shifts in kinetic parameters can be investigated after the addition of enhancers or inhibitors, which further characterises their activity (competitive, non-competitive and uncompetitive) as exemplified by Tropolone as a non-competitive inhibitor. Although we determined that the used extract was enriched in CRL1 and CRL3 through MS analysis, the determined kinetic parameters are specific for this particular extract composition. In conclusion, each isoform needs to be investigated individually to acquire specific kinetic parameters.

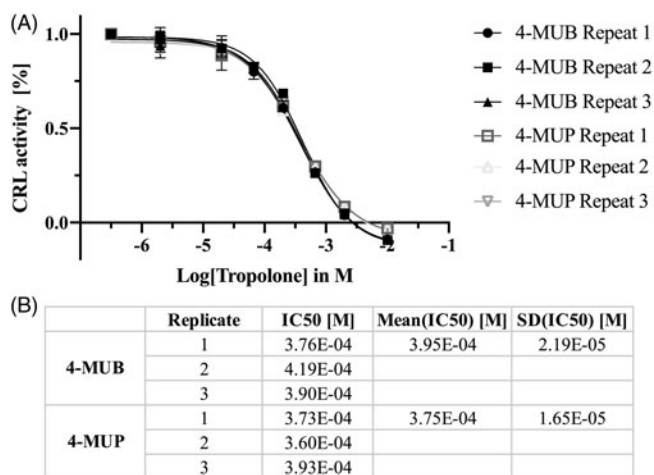


Figure 4. Analysis of Tropolone's inhibitory effect on CRL activity in the developed enzyme activity assay with 4-MUP and 4-MUB. (A) Plot of replicated IC_{50} curves for 4-MUP and 4-MUB with Tropolone concentrations between 2 μM and 10 mM. (B) Analysis and determination of the IC_{50} values for both substrates. IC_{50} values were determined by plotting the logarithmic Tropolone concentration against the percentage of CRL activity, which allows the determination of IC_{50} values: 4-MUP: 3.75×10^{-4} M; 4-MUB: 3.95×10^{-4} M and standard deviations of 1.65×10^{-5} and 2.19×10^{-5} , respectively.

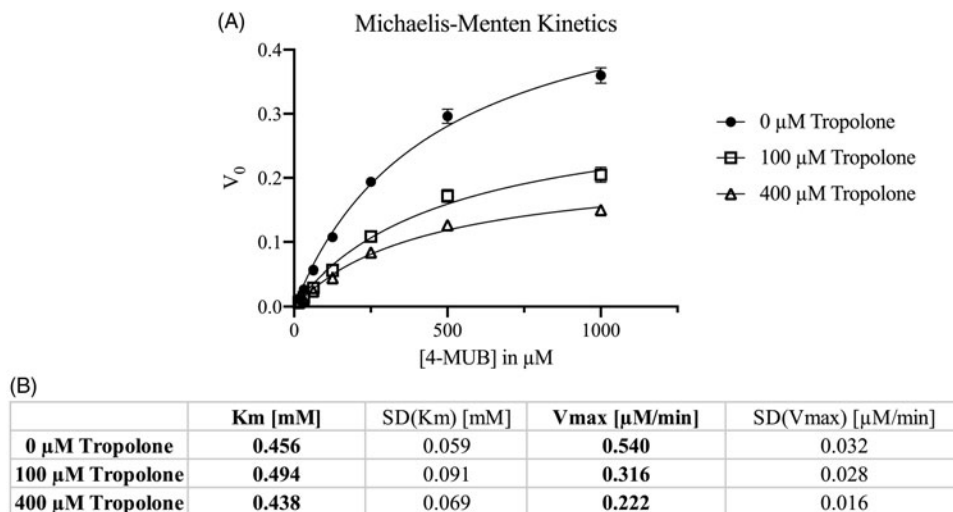


Figure 5. Michaelis-Menten kinetics to investigate the performance of CRL with the in-house developed enzyme activity assay and various 4-MUB concentrations over time. We used 0, 100, or 400 μM Tropolone in the experiment to measure the impact on V_{max} and K_m by the inhibitor. While K_m was maintained after inhibitor addition, V_{max} was decreasing with increasing inhibitor concentration. Therefore, our results suggest that Tropolone is a non-competitive inhibitor.

Moreover, the assay was used to verify the impact of the new *in-silico* determined allosteric modulator Tropolone on CRL activity. Tropolone is a seven-carbon aromatic ring, which is a common motif in naturally occurring compounds. It was shown to inhibit the grape polyphenol oxidase as well as the mushroom tyrosinase^{29,30}. So far, it has not been reported that Tropolone can inhibit lipases, although other natural compound classes such as flavonoids, alkaloids, and saponins are known to inhibit CRL's activity with varying efficacy depending on the used concentration^{25,26}.

Both assays, 4-MUP and 4-MUB, were tested to show that CRL's activity is inhibited by Tropolone in a concentration-dependent manner. The substrate independent inhibition and the similarity of the determined IC50s indicate that Tropolone could interfere with CRL's enzymatic activity, which has been further investigated by biolayer-interferometry and Michaelis–Menten kinetics. The results suggested that Tropolone is a non-competitive inhibitor. Given the slight differences in the assay conditions between 4-MUB and 4-MUP, we were not able to directly compare the efficiency of Tropolone in inhibiting CRL in those assays. However, each assay individually is inter-comparable between runs and samples and can be applied for high-throughput screening.

Finally, to validate our enzyme activity assay performance, in comparison to IC50s of the published CRL inhibitors Berberine, β -Aescin and Trigonelline (which had been determined by high-performance liquid chromatography (HPLC)), we measured the IC50s of the published compounds in our assay^{25,26}. The selected inhibitors showed similar IC50s in the enzyme activity assay as compared to the HPLC method, which confirmed the assays competitiveness.

In addition, using biolayer-interferometry to determine the K_D of Tropolone, Trigonelline and β -Aescin, Tropolone showed the most specific interaction with the strongest K_D , while Trigonelline and β -Aescin indicated weaker K_D s and/or unspecific interaction with the enzyme. Although the results are partly different from the enzyme activity assay's results, the two assays investigate different parameters: activity and interaction. Our results highlight Tropolone's mode of action as non-competitive CRL inhibitor and that our newly developed assay is comparable to other methods such as HPLC.

5. Conclusion

The miniaturised *in-vitro* assay we have developed proved to be reliable, robust, and delivered reproducible results and was subsequently used to verify an *in-silico* determined allosteric modulator. Furthermore, our study demonstrated that the application of *in-silico* screening together with an *in-vitro* fluorescence assay aided the identification of a new non-competitive inhibitor of *Candida rugosa* lipase. The assay enabled the characterisation of the used enzyme extract through the determination of kinetic parameters and product quality. In future application, the assay could be used to investigate and characterise other enzymes and enzyme classes and could be included in automated processes. Both methods together, *in-silico* and *in-vitro* screening, represent an alternative to standard high-throughput approaches and resulted in the identification of the non-competitive CRL inhibitor, 'Tropolone', which could have pharmacological potential.

Disclosure statement

The authors report no conflict of interest.

Funding

This work was supported by the Roskamp Institute Inc. and by a Sponsored Research Agreement between The Roskamp Institute, Inc and Enzymedica, Inc.

ORCID

Ariane Menden  <http://orcid.org/0000-0002-0108-6243>

Davane Hall  <http://orcid.org/0000-0002-5063-1666>

Venkatarian Mathura  <http://orcid.org/0000-0003-3337-7122>

Michael Mullan  <http://orcid.org/0000-0002-1473-7527>

Ghania Ait-Ghezala  <http://orcid.org/0000-0002-9836-8617>

References

1. Barriuso J, Vaquero ME, Prieto A, et al. Structural traits and catalytic versatility of the lipases from the *Candida rugosa*-like family: a review. *Biotechnol Adv* 2016;34:874–85.
2. Kolattukudy PE. Enzymatic penetration of the plant cuticle by fungal pathogens. *Annu Rev Phytopathol* 1985; 23: 223–50.
3. Lotti M, Tramontano A, Longhi S, et al. Variability within the *Candida rugosa* lipases family. *Protein Eng* 1994;7:531–5.
4. Xu M-H, Kuan I-C, Deng F-Y, et al. Immobilization of lipase from *Candida rugosa* and its application for the synthesis of biodiesel in a two-step process. *Asia-Pac J Chem Eng* 2016; 11:910–7.
5. Hongwei Y, Jinchuan W, Chi Bun C. Kinetic resolution of ibuprofen catalyzed by *Candida rugosa* lipase in ionic liquids. *Chirality* 2005;17:16–21.
6. Laguerre M, Nlandu Mputu M, Briys B, et al. Regioselectivity and fatty acid specificity of crude lipase extracts from *Pseudozyma tsukubaensis*, *Geotrichum candidum*, and *Candida rugosa*. *Eur J Lipid Sci Techn* 2017;119:1600302.
7. Brocca S, Secundo F, Ossola M, et al. Sequence of the lid affects activity and specificity of *Candida rugosa* lipase iso-enzymes. *Protein Sci* 2009;12: 2312–9.
8. Redondo O, Herrero A, Bello JF, et al. Comparative kinetic study of lipases A and B from *Candida rugosa* in the hydrolysis of lipid p-nitrophenyl esters in mixed micelles with Triton X-100. *Biochim Biophys Acta* 1995;1243:15–24.
9. Akoh CC, Lee GC, Shaw JF. Protein engineering and applications of *Candida rugosa* lipase isoforms. *Lipids* 2004;39: 513–26.
10. Schmitt J, Brocca S, Schmid RD, et al. Blocking the tunnel: engineering of *Candida rugosa* lipase mutants with short chain length specificity. *Protein Eng* 2002;15: 595–601.
11. Grochulski P, Bouthillier F, Kazlauskas RJ, et al. Analogs of reaction intermediates identify a unique substrate binding site in *Candida rugosa* lipase. *Biochemistry* 1994;33: 3494–500.
12. Grochulski P, Li Y, Schrag JD, et al. Two conformational states of *Candida rugosa* lipase. *Protein Sci* 2008;3:82–91.
13. Cygler MG, Grochulski P, Schrag J. Substrate binding site and the role of the flap loop in *Candida Rugosa* lipase, a close relative of acetylcholinesterase. New York: Springer Science and Business Media; 1995.
14. Herbst D, Peper S, Niemeyer B. Enzyme catalysis in organic solvents: influence of water content, solvent composition and temperature on *Candida rugosa* lipase catalyzed transesterification. *J Biotechnol* 2012;162: 398–403.

15. Kahveci D, Xu X. Enhancement of activity and selectivity of *Candida rugosa* lipase and *Candida antarctica* lipase A by bioimprinting and/or immobilization for application in the selective ethanolysis of fish oil. *Biotechnol Lett* 2011;33:2065–71.
16. Sri Kaja B, Lumor S, Besong S, et al. Investigating Enzyme Activity of Immobilized *Candida rugosa* Lipase. *J Food Qual* 2018;2018:1–9.
17. Pereira EB, De Castro HF, De Moraes FF, et al. Esterification activity and stability of *Candida rugosa* lipase immobilized into chitosan. *Appl Biochem Biotechnol* 2002;98–100:977–86.
18. Mozaffar Z, Weete JD. Invert emulsion as a medium for fungal lipase activity. *J Am Oil Chemist Soc* 1995;72:1361–6.
19. Mancheno JM. Structural insights into the lipase/esterase behavior in the *Candida rugosa* lipases family: crystal structure of the lipase 2 isoenzyme at 1.97Å resolution. *J Mol Biol* 2003;332:1059–69.
20. Friesner RA, Banks JL, Murphy RB, et al. Glide: a new approach for rapid, accurate docking and scoring. 1. Method and assessment of docking accuracy. *J Med Chem* 2004;47:1739–49.
21. Halgren TA, Murphy RB, Friesner RA, et al. Glide: a new approach for rapid, accurate docking and scoring. 2. Enrichment factors in database screening. *J Med Chem* 2004;47:1750–9.
22. Friesner RA, Murphy RB, Repasky MP, et al. Extra precision glide: docking and scoring incorporating a model of hydrophobic enclosure for protein-ligand complexes. *J Med Chem* 2006;49:6177–96.
23. Dairaku T, Iwamoto T, Nishimura M, et al. A practical fluorometric assay method to measure lysosomal acid lipase activity in dried blood spots for the screening of cholesteryl ester storage disease and Wolman disease. *Mol Genet Metab* 2014;111:193–6.
24. Palocci C, Falconi M, Alcaro S, et al. An approach to address *Candida rugosa* lipase regioselectivity in the acylation reactions of trytilated glucosides. *J Biotechnol* 2007; 128:908–18.
25. Grippa E, Valla R, Battinelli L, et al. Inhibition of *Candida rugosa* lipase by berberine and structurally related alkaloids, evaluated by high-performance liquid chromatography. *Biosci Biotechnol Biochem* 1999;63:1557–62.
26. Ruiz C, Falcocchio S, Xoxi E, et al. Inhibition of *Candida rugosa* lipase by saponins, flavonoids and alkaloids. *J Mol Catal B Enzym* 2006;40:138–43.
27. Pimentel MCB, Leao ABF, Melo EHM, et al. Immobilization of *Candida rugosa* lipase on magnetized Dacron: kinetic study. *Artif Cells Blood Substit Immobil Biotechnol* 2007;35:221–35.
28. Gupta PK, Sastry KV. Effect of mercuric chloride on enzyme activities in the digestive system and chemical composition of liver and muscles of the catfish, *Heteropneustes fossilis*. *Ecotoxicol Environ Saf* 1981;5:389–400.
29. Valero E, Garcia-Moreno M, Varon R, et al. Time-dependent inhibition of grape polyphenol oxidase by tropolone. *J Agric Food Chem* 1991;39:1043–6.
30. Espin JC, Wichers HJ. Slow-binding inhibition of mushroom (*Agaricus bisporus*) tyrosinase isoforms by tropolone. *J Agric Food Chem* 1999;47:2638–44.